TIME-TO-DEPTH MAPPING AND IMAGING OF TIME-MIGRATED SEISMIC DATA WITH INHERENT VELOCITY ESTIMATION: REVISITED

E. Iversen and M. Tygel

email: *mtygel@gmail.com*

keywords: *Time migration, image rays, time-to-depth mapping, time-to-depth imaging*

ABSTRACT

We extend the paper with the same title that composes the WIT Report 2006. The new material includes an updated description of our depth-velocity determination algorithm and the incorporation of a 3D synthetic example. Our results show that the method works well in the present 3D situation.

INTRODUCTION

This work is a continuation of our previous paper, Iversen and Tygel (2006), from now on referred to as Paper I. Our objective is to present theory and numerical examples for a 3D image-ray tracing and depth-velocity estimation algorithm. As also indicated in Paper I, we rely on the analysis and many results of the pioneering works of Cameron et al. (2006) in 2D and Cameron et al. (2007) in 3D. It differs, however, in the algorithm of image-ray tracing and the construction of depth velocities. The algorithm presented in Cameron et al. (2007) requires that the time-migrated velocity field is available for at least three different directions along the measurement surface. Our algorithm uses requires only one direction for the time-migrated velocity field. As a consequence, the range of practical applications is extended. A discussion on the actual differences between the two approaches is provided in Appendix A.

In order to have the paper self contained, we review the methodology and main results of Paper I. In the process, we also update some of the explanations and expressions.

The new algorithm has been applied and discussed on a 3D synthetic example. Our overall impression from this first test is that the errors generated by the developed image-ray transformation are smaller than those of the classic vertical-ray transformation, in particular concerning lateral positioning.

NOMENCLATURE

In order to make the mathematical derivations easier to follow, lists of the most important symbols used in the text are displayed in Table 1. Lower and upper case letters, i and I, used as subscripts may have the values $i = 1, 2, 3$, and $I = 1, 2$, respectively. For three-component vectors we use standard notation, e.g., $\mathbf{a}$, while for two-component vectors a bar is written above the symbol, e.g., $\bar{\mathbf{a}}$. Vectors are equivalently considered as column matrices. To distinguish between matrices of size 3×3 and 2×2, we use the notations $\hat{\mathbf{A}}$ and $\mathbf{A}$, respectively. The notation $\mathbf{A}^T$ is used for the transpose of the matrix $\mathbf{A}$, while $\mathbf{A}^{-T}$ is a shorthand notation for ${\mathbf{A}^{-1}}^T$. In cases where ambiguity may arise, a superscript in the form (q) on vectors/matrices serves as a label for the coordinate system under consideration. The 3×1 column vector containing the first partial derivatives and the 3×3 matrix containing the second-order partial derivatives of a scalar field W with respect to the variables, $\mathbf{x} = (x_i)$, are written in the forms

$$\frac{\partial W}{\partial \mathbf{x}} = \left(\frac{\partial W}{\partial x_i}\right)^T \quad \text{and} \quad \frac{\partial^2 W}{\partial \mathbf{x}^2} = \left(\frac{\partial^2 W}{\partial x_i \partial x_j}\right) . \tag{1}$$

Symbol	Meaning
$\mathbf{x} = (x_i)$	Global Cartesian coordinates of the depth domain
$\bar{\mathbf{s}}, \bar{\mathbf{r}}, \quad \bar{\mathbf{x}} = (\bar{\mathbf{s}} + \bar{\mathbf{r}})/2, \bar{\mathbf{y}} = (\bar{\mathbf{s}} - \bar{\mathbf{r}})/2$	Source/receiver and midpoint/half-offset coordinates at measurement surface
$\bar{\mathbf{x}}^M, \mathbf{a} = \bar{\mathbf{x}} - \bar{\mathbf{x}}^M$	Time-migration apex and aperture vectors at measurement surface
t	Time variable of the unmigrated time domain
T^M	Time variable of the migrated time domain
$(\bar{\mathbf{x}}, t)$	Unmigrated time domain coordinates
$(\bar{\mathbf{x}}^M, T^M)$	Migrated time domain coordinates
θ	Migration azimuth
$\bar{\mathbf{u}} = (\cos\theta, \sin\theta)^T$	Unit vector in the migration azimuth direction
$\boldsymbol{\gamma} = (\gamma_i), \gamma_I = x_I^M, \gamma_3 = T = T^M/2$	Ray coordinates for a field of image rays
$\mathbf{q} = (q_i)$	Local Cartesian coordinates along the image ray
$(\bar{\mathbf{q}}, \gamma_3), \gamma_3 = T$	Ray-centered coordinates along the image ray
$V^M(\bar{\mathbf{x}}^M, T^M)$	Time-migration velocity field for a given migration azimuth
$v^M_{dix}(\boldsymbol{\gamma})$	Time-migration interval velocity field for a given migration azimuth
$v(\mathbf{x}), v(\mathbf{q})$	Depth-domain velocity field in global and local Cartesian coordinates
$V(\boldsymbol{\gamma})$	Depth-domain velocity field in ray coordinates
$F(\boldsymbol{\gamma})$	Velocity spreading factor
$\hat{\mathbf{M}}^{(x)}$	3×3 symmetric matrix corresponding to azimuth-dependent migration velocity
$\mathbf{x}, \mathbf{p}$	Position and slowness vectors of image rays
$\mathbf{x}^0, \mathbf{p}^0, v^0, \mathbf{e}_1^0, \boldsymbol{\Pi}^0$ and $\boldsymbol{\gamma}^0$	Image-ray quantities at the initial point $\boldsymbol{\gamma}^0 = (x_I^{M0}, t^{MO} = 0)$
$\hat{\mathbf{Q}}_1^{(x)}, \hat{\mathbf{Q}}_1^{(q)}$	3×3 matrices $(\partial x_i/\partial\gamma_j)$ and $(\partial q_i/\partial\gamma_j)$, in global and local Cartesian coordinates, corresponding to plane-wave initial condition
$\boldsymbol{\Pi}$	Ray propagator matrix
$\mathbf{Q}_1, \mathbf{P}_1$	First set of paraxial matrices, corresponding to plane-wave initial condition
$\mathbf{Q}_2, \mathbf{P}_2$	Second set of paraxial matrices, corresponding to point-source initial condition
$\mathbf{H} = (\mathbf{e}_1\ \mathbf{e}_2\ \mathbf{e}_3)$	3×3 transformation matrix with columns $\mathbf{e}_i$, the i-th unit vector of the local Cartesian coordinate system along the image ray

Table 1: Table of most important symbols used in the text.

THEORY

In this section, we explain how we can trace image rays into depth and simultaneously estimate the velocity along them from the knowledge of a 3D time-migration velocity field in an arbitrary single direction along the measurement surface. We observe that the required single-direction velocities are extracted from an underlying full 3D time-migration velocity field.

Coordinate systems: The construction of image rays, as envisaged by our methodology, mainly relies on the concepts and results of standard kinematic and dynamic ray tracing, as described, e.g. in Červený (2001). In this way, it is instrumental to introduce, besides a global depth-domain Cartesian coordinate system, $\mathbf{x} = (x_i)$, also additional coordinate systems that will be associated to the image rays. The first of these to be mentioned here is the coordinate system associated with the time-migration domain, (x_1^M, x_2^M, T^M). Closely connected to the latter is the *ray coordinate system*, $\boldsymbol{\gamma} = (\gamma_i)$, which defines the image rays issued from all trace locations of the time-migrated seismic data set. This means that that the first two coordinates are defined as $\gamma_1 = x_1^M$, $\gamma_2 = x_2^M$. For the variable along the ray, γ_3, we shall use the one-way traveltime, denoted by the symbol T. In other words, we have $\gamma_3 = T = T^M/2$. The three-dimensional curvilinear space formed by the ray coordinates is referred to as the *ray domain*. Finally, we shall need also the *ray-centered coordinate system*, (q_1, q_2, γ_3), introduced by Popov and Pšenčík (1978) and a corresponding local Cartesian coordinate system, $\mathbf{q} = (q_i)$, which is attached to each individual point on the image ray. The vectorial function $\mathbf{x}(\boldsymbol{\gamma})$ describes a mapping of a point $\boldsymbol{\gamma}$ in the ray coordinate system

onto a point $\mathbf{x}$ in the global Cartesian coordinate system. Since this mapping is based on the construction of image rays, we refer to it as the *image-ray transformation*.

Input data: For the combined image-ray tracing and depth-domain velocity estimation, we assume the knowledge of a single-direction time-migration velocity function, $V^M = V^M(\bar{\mathbf{x}}^M, T^M, \theta)$, extracted from a full 3D time-migration velocity field. Here, $\bar{\mathbf{x}}^M = (x_1^M, x_2^M)^T$ specifies a trace in the time-migrated data set, T^M denotes the (two-way) migration time and θ is the angle specifying the direction along which the migration velocity is given. This angle is referred to in the following as the *migration azimuth* or, in brief, just as azimuth.

Prior to applying our ray-tracing method, it is practical to convert the time-migration velocity by Dix's method to the so-called *time-migration interval velocity*,

$$v_{dix}^M(\boldsymbol{\gamma}) = \left\{ \frac{d}{dT^M}[T^M (V^M)^2] \right\}^{1/2} = \left\{ \frac{d}{dT}[T (V^M)^2] \right\}^{1/2} . \tag{2}$$

The function v_{dix}^M must possess only weak variations with respect to the (lateral) coordinates γ_1 and γ_2. In addition, it is essential for the stability of the ray-tracing procedure that v_{dix}^M and its derivatives $\partial v_{dix}^M / \partial \gamma_i$ and $\partial^2 v_{dix}^M / (\partial \gamma_I \partial \gamma_J)$ are smooth functions of all three coordinates γ_i.

Kinematic ray tracing: A basis for kinematic ray tracing in 3D isotropic elastic media can be formulated by the ordinary differential equations (see, e.g., Červený, 2001, Section 3.1.1)

$$\frac{d\mathbf{x}}{dT} = v^2(\mathbf{x})\mathbf{p}, \qquad \text{and} \qquad \frac{d\mathbf{p}}{dT} = -\, v^{-1}(\mathbf{x}) \frac{\partial v}{\partial \mathbf{x}}. \tag{3}$$

Evaluation of the above kinematic ray-tracing equations requires the knowledge of the velocity, $V(\mathbf{x})$ and its gradient, $\partial v / \partial \mathbf{x}$, which we do not have directly access to. As shown below, however, we will overcome this situation by a further analysis that involves the dynamic ray-tracing system.

Dynamic ray tracing: The dynamic ray-tracing system, also in 3D isotropic elastic media, is now formulated in ray-centered coordinates. For a fixed image ray, we consider the attached local Cartesian coordinate system, $\mathbf{q}$. For each coordinate, q_i, we associate a corresponding unit basis vector, $\mathbf{e}_i$. These unit vectors constitute the columns of an orthonormal transformation matrix,

$$\hat{\mathbf{H}} = \begin{pmatrix} \mathbf{e}_1 & \mathbf{e}_2 & \mathbf{e}_3 \end{pmatrix} . \tag{4}$$

The matrix $\hat{\mathbf{H}}$ can be computed in any point along the ray if we include within the system of ray differential equations the following equation,

$$\frac{d\mathbf{e}_1}{dT} = -\, v^2 (\mathbf{e}_1 \cdot \frac{d\mathbf{p}}{dT}) \mathbf{p} \, , \tag{5}$$

where $d\mathbf{p}/dT$ is given by the second relation in equation 3. Knowing the vector $\mathbf{e}_3 = \mathbf{p}/\|\mathbf{p}\|$ and in addition the vector $\mathbf{e}_1$ resulting from numerical integration including equation 5, the vector $\mathbf{e}_2$ is easily obtained by the cross product

$$\mathbf{e}_2 = \mathbf{e}_3 \times \mathbf{e}_1 \, . \tag{6}$$

In the following, we use the standard formulation of complete dynamic ray tracing in terms of 4×4 matrices in ray-centered coordinates,

$$\frac{d\boldsymbol{\Pi}}{dT} = \mathbf{S}\boldsymbol{\Pi} \, , \tag{7}$$

with the initial condition

$$\boldsymbol{\Pi}^0 = \begin{pmatrix} \mathbf{I} & \mathbf{0} \\ \mathbf{0} & \mathbf{I} \end{pmatrix} . \tag{8}$$

Here, $\boldsymbol{\Pi}$ is the ray propagator matrix with sub-matrices of size 2×2,

$$\boldsymbol{\Pi} = \begin{pmatrix} \mathbf{Q}_1 & \mathbf{Q}_2 \\ \mathbf{P}_1 & \mathbf{P}_2 \end{pmatrix} . \tag{9}$$

As is well-known, the first and second set of paraxial matrices, $(\mathbf{Q}_1, \mathbf{P}_1)$ and $(\mathbf{Q}_2, \mathbf{P}_2)$, can be interpreted as *plane-wave (or telescopic)* and *point-source* components of the propagator matrix, $\mathbf{\Pi}$ (see, e.g., Červený, 2001). Since image rays correspond to an initially plane wave, the relevant set of paraxial matrices is $(\mathbf{Q}_1, \mathbf{P}_1)$. Matrix $\mathbf{S}$ in equation 7 has the definition

$$\mathbf{S} = \begin{pmatrix} \mathbf{0} & v^2\mathbf{I} \\ -v^{-1}\mathbf{V} & \mathbf{0} \end{pmatrix}, \quad \text{where} \quad \mathbf{V} = \left(\frac{\partial^2 v}{\partial q_I \partial q_J} \right). \tag{10}$$

Relating time- and depth-domain velocity functions: In order to simplify the notation, we shall, in the following, consider three velocity functions, all of them denoted by the letter, v, and distinguished solely by their arguments: $v(\mathbf{x})$, $v(\boldsymbol{\gamma})$ and $v(\mathbf{q})$. More specifically, $v(\mathbf{x})$ and $v(\boldsymbol{\gamma})$ will designate the depth-domain velocity in global Cartesian coordinates and ray coordinates, respectively. In a standard forward ray-tracing application, i.e., when image rays are computed from a known velocity field $v(\mathbf{x})$, the velocity $v(\boldsymbol{\gamma})$ can be obtained for each ray (for which the first two components, $\bar{\boldsymbol{\gamma}} = (\gamma_1, \gamma_2)^T$ are fixed) simply by assigning the value $v(\mathbf{x})$ at each position $\mathbf{x}$ on the ray to the corresponding coordinate vector $\boldsymbol{\gamma}$. Finally, for any selected point on the ray, $v(\mathbf{q})$ defines the velocity in the local Cartesian coordinate system.

As shown in Appendix B, the ray-domain velocity, $V(\boldsymbol{\gamma})$, will be given by

$$V(\boldsymbol{\gamma}) = v^M_{dix}(\boldsymbol{\gamma}) F(\boldsymbol{\gamma}), \tag{11}$$

where F, referred to as the *velocity spreading factor*, is given by

$$F(\boldsymbol{\gamma}) = \frac{\bar{\mathbf{u}}^T {\mathbf{Q}_2}^{-1} \mathbf{Q}_1 \bar{\mathbf{u}}}{\left\{ \bar{\mathbf{u}}^T \mathbf{Q}_2^{-1} \mathbf{Q}_2^{-T} \bar{\mathbf{u}} \right\}^{1/2}}. \tag{12}$$

In the 2D situation, the factor F reduces to the simple formula

$$F(\boldsymbol{\gamma}) = Q_1, \tag{13}$$

where Q_1 is the scalar that corresponds, in 2D propagation, to the 2×2 transformation matrix, $\mathbf{Q}_1$, which refers to the 3D situation. Expression 13 coincides with the one given in Cameron et al. (2006, 2007).

We note that, although v^M_{dix} is directly available as input, the factor F depends on quantities belonging to dynamic ray tracing along the image ray. This means that our image-ray construction must contemplate a simultaneous solution of the kinematic and dynamic ray-tracing systems.

Derivatives of velocity functions: We now address the problem of determining the velocity derivatives $\partial V / \partial \mathbf{x}$ and $\partial^2 v / \partial \bar{\mathbf{q}}^2$ that are needed in the kinematic and dynamic ray-tracing systems formulated above. These will be given in terms of the ray-domain velocity derivatives, $\partial v / \partial \boldsymbol{\gamma}$ and $\partial^2 v / \partial \bar{\boldsymbol{\gamma}}^2$, respectively. The latter derivatives are, in turn, closely related to the corresponding derivatives of our input time-migration interval velocity field, v^M_{dix}.

For first-order derivatives, a simple application of the chain rule of advanced calculus yields

$$\frac{\partial V}{\partial \gamma_i} = \frac{\partial x_k}{\partial \gamma_i} \frac{\partial v}{\partial x_k}, \tag{14}$$

and also introduces the matrix

$$\hat{\mathbf{Q}}_1^{(x)} = \left(\frac{\partial x_i}{\partial \gamma_j} \right) \tag{15}$$

of the transformation between ray coordinates (γ_i) and global Cartesian coordinates (x_k). Furthermore, one can relate matrix $\hat{\mathbf{Q}}_1^{(x)}$ to its counterpart, $\hat{\mathbf{Q}}_1^{(q)} = (\partial q_i / \partial \gamma_j)$, in local Cartesian coordinates by the transformation

$$\hat{\mathbf{Q}}_1^{(x)} = \hat{\mathbf{H}} \hat{\mathbf{Q}}_1^{(q)}, \quad \text{where} \quad \hat{\mathbf{Q}}_1^{(q)} = \begin{pmatrix} \mathbf{Q}_1 & \begin{matrix} 0 \\ 0 \end{matrix} \\ \begin{matrix} 0 & 0 \end{matrix} & v \end{pmatrix}. \tag{16}$$

We recall that $\hat{\mathbf{H}}$ is the 3×3 matrix given by equation 4 and $\mathbf{Q}_1$ is the 2×2 upper left submatrix of the 4×4 ray-centered propagator matrix, $\mathbf{\Pi}$, of equation 9. Under the assumption that the inverse matrix, $(\hat{\mathbf{Q}}_1^{(x)})^{-1} = (\partial\gamma_i/\partial x_j)$, exists (or equivalently, that $\det \hat{\mathbf{Q}}^{(x)} \neq 0$), equation 14 can be recast as

$$\frac{\partial v}{\partial \mathbf{x}} = (\hat{\mathbf{Q}}_1^{(x)})^{-T} \frac{\partial V}{\partial \boldsymbol{\gamma}} \, . \tag{17}$$

The existence of the inverse matrix $(\hat{\mathbf{Q}}_1^{(x)})^{-1}$ for all considered values of the ray-coordinate vector $\boldsymbol{\gamma}$ ensures a one-to-one correspondence between ray coordinates and depth-domain coordinates, $\mathbf{x} = \mathbf{x}(\boldsymbol{\gamma})$ and $\boldsymbol{\gamma} = \boldsymbol{\gamma}(\mathbf{x})$. Thus, in this particular situation each point in the depth domain is connected to the measurement surface by at most one image ray only, and the image-ray field does not contain caustic points. We remark, in passing, that the condition $\det \hat{\mathbf{Q}}_1^{(x)} \neq 0$ has to be fulfilled in any implementation of the image-ray construction considered here. To obtain the relationship between the second derivatives of velocity in ray coordinates and local Cartesian coordinates, the chain rule needs to be applied twice. As shown in Appendix C, we have

$$\frac{\partial^2 V}{\partial q_N \partial q_M} = \frac{\partial \gamma_I}{\partial q_N} \frac{\partial \gamma_J}{\partial q_M} \left(\frac{\partial^2 V}{\partial \gamma_I \partial \gamma_J} - \frac{\partial^2 q_K}{\partial \gamma_I \partial \gamma_J} \frac{\partial V}{\partial q_K} \right) + M_{NM} \frac{\partial V}{\partial T} \, , \tag{18}$$

where $M_{NM} = \partial^2 T / \partial q_N \partial q_M$. At this point, it is essential to emphasize that conventional dynamic ray tracing for a single ray does not allow computation of derivatives of q_K of order two and higher. Hence, we can conclude that if the procedure is to be based on computations along a single ray only, we have to make the assumption that such derivatives have negligible values. Given that this assumption is satisfied, equation 18 can be approximated by the simpler matrix expression

$$\frac{\partial^2 V}{\partial \bar{\mathbf{q}}^2} = \mathbf{Q}_1^{-T} \frac{\partial^2 V}{\partial \bar{\boldsymbol{\gamma}}^2} \mathbf{Q}_1^{-1} + \mathbf{M}_1 \frac{\partial V}{\partial T} \, , \tag{19}$$

where $\mathbf{M}_1 = \partial^2 T / \partial \bar{\mathbf{q}}^2 = \mathbf{P}_1 \mathbf{Q}_1^{-1}$. Equations 17 and 18 (or equation 19) provide the link between the first and second derivatives of velocity with respect to ray coordinates and the corresponding velocity derivatives with respect to global Cartesian coordinates and ray-centered coordinates, respectively. As seen in the next section, this link will be crucial for the image-ray tracing and velocity estimation algorithm that is proposed here.

Numerical integration along the image ray: Collecting results, the complete set of ordinary differential equations integrated to obtain the image ray is specified by equations 3, 5, and 7. As input to the evaluation of the right-hand side of the differential equations, we have the independent variable along the ray, T, and the set of dependent variables, $\mathbf{x}$, $\mathbf{p}$, $\mathbf{e}_1$, and $\mathbf{\Pi}$. We also need as input the horizontal coordinates of the starting point of the image ray, x_I^{M0}, the unit vector corresponding to the migration azimuth, $\bar{\mathbf{u}}$, and the time-migration interval velocity field, $v_{dix}^M(\boldsymbol{\gamma})$. An important part of the procedure is on-the-fly transformation of function values, first derivatives, and second derivatives belonging to the time-migration interval velocity field, $v_{dix}^M(\boldsymbol{\gamma})$, to corresponding quantities in the ray-domain velocity field, $V(\boldsymbol{\gamma})$. For a better appreciation of the numerical integration scheme that is central to our time-to-depth conversion algorithm, we have specified in Table 2 the sequence of computational operations involved in the evaluation of the differential equations. It has been assumed that derivatives along a ray of ray-centered coordinates, q_K, of higher order than one in the ray parameters, γ_I, can be neglected. For the isotropic conditions under consideration, the ray-domain velocity can be obtained, besides from equation 11, as the inverse length of the slowness vector, $V = \|\mathbf{p}\|^{-1}$. This provides a possibility of checking the numerical accuracy during integration of the differential equations. For details concerning computation of velocity derivatives along the image ray, see Appendix D.

Initial conditions for tracing the image ray: In order solve the kinematic and dynamic ray-tracing systems, initial conditions have to be provided. These consist of initial values, $\mathbf{x}^0$, $\mathbf{p}^0$, ${\mathbf{e}_1}^0$, and $\mathbf{\Pi}^0$, given for the initial ray coordinate vector $\boldsymbol{\gamma}^0 = (\gamma_1^0, \gamma_2^0, \gamma_3^0)^T$. Assuming, for simplicity, a planar horizontal

Step #	Description	Equation #
1	Form the vector $\boldsymbol{\gamma} = (\gamma_1, \gamma_2, T)^T$, where $\gamma_1 = x_1^{M0}$ and $\gamma_2 = x_2^{M0}$ are fixed for all computations along the ray.	
2	Evaluate the time-migration interval velocity, v_{dix}^M , and its derivatives, $\partial v_{dix}^M/\partial\gamma_I$ and $\partial^2 v_{dix}^M/\partial\gamma_I\partial\gamma_J$.	
3	Calculate the factors A, B, and F: $A = \bar{\mathbf{u}}^T\mathbf{Q}_2^{-1}\mathbf{Q}_1\bar{\mathbf{u}}$ and $B = \bar{\mathbf{u}}^T\mathbf{Q}_2^{-1}\mathbf{Q}_2^{-T}\bar{\mathbf{u}}$, $F = A/B^{1/2}$.	53 54
4	Establish the depth-domain velocity, $V = v_{dix}^M\ F$.	11
5	Evaluate the differential equations $d\mathbf{x}/dT = v^2\mathbf{p}$, $d\mathbf{Q}_I/dT = v^2\mathbf{P}_I$.	3 7, 9, 10
6	Find the two remaining basis vectors of the local Cartesian coordinate system, using $\mathbf{e}_3 = \mathbf{p}/\|\mathbf{p}\|$ and $\mathbf{e}_2 = \mathbf{e}_3 \times \mathbf{e}_1$. This yields the transformation matrix $\hat{\mathbf{H}} = (\mathbf{e}_1\ \mathbf{e}_2\ \mathbf{e}_3)$.	6 4
7	Use the transformation $\hat{\mathbf{Q}}^{(x)} = \hat{\mathbf{H}}\hat{\mathbf{Q}}^{(q)}$.	16
8	Find derivatives of the factors A, B, and F, using the equations $\partial A/\partial T = -V^2\bar{\mathbf{u}}^T\mathbf{Q}_2{}^{-1}\mathbf{Q}_2{}^{-T}\bar{\mathbf{u}} = -V^2\,B$ $\partial B/\partial T = -2V^2\bar{\mathbf{u}}^T\mathbf{Q}_2{}^{-1}\mathbf{P}_2\mathbf{Q}_2{}^{-1}\mathbf{Q}_2{}^{-T}\bar{\mathbf{u}}$. $\partial F/\partial T = (\partial A/\partial T)\,B^{1/2} - (\partial B/\partial T)\,(A/2)B^{-3/2}$.	55 55 54
9	Apply approximations for derivatives of factor F along the ray, which yields $\partial V/\partial\gamma_I = \partial v_{dix}^M/\partial\gamma_I\ F$ and $\partial V/\partial T = \partial v_{dix}^M/\partial T\ F + v_{dix}^M\ \partial F/\partial T$.	52
10	Obtain the velocity gradient in depth-domain Cartesian coordinates by $\partial v/\partial\mathbf{x} = (\hat{\mathbf{Q}}^{(x)})^{-T}\ \partial V/\partial\boldsymbol{\gamma}$.	17
11	Evaluate the differential equations for the vectors $\mathbf{p}$ and $\mathbf{e}_1$, $d\mathbf{p}/dT = -v^{-1}\ \partial v/\partial\mathbf{x}$, $d\mathbf{e}_1/dT = -v^2\ (\mathbf{e}_1\cdot\ d\mathbf{p}/dT)\ \mathbf{p}$.	3 5
12	Find the approximate second derivatives $\partial^2 V/\partial\gamma_I\partial\gamma_J\ = (\partial^2 v_{dix}^M/\partial\gamma_I\partial\gamma_J)\ F$, and apply the transformation $\partial^2 V/\partial\bar{\mathbf{q}}^2 = \mathbf{Q}_1^{-T}(\partial^2 V/\partial\bar{\boldsymbol{\gamma}}^2)\mathbf{Q}_1^{-1} + \mathbf{M}_1(\partial V/dT)$, with $\mathbf{M}_1 = \mathbf{P}_1\mathbf{Q}_1^{-1}$.	52 49
13	As a final step, evaluate the differential equations for matrices $\mathbf{P}_I$ by $d\mathbf{P}_I/dT = -v^{-1}\mathbf{V}\mathbf{Q}_I$.	7, 9, 10

Table 2: Proposed sequence of computational steps involved in the evaluation of the right-hand side of the system of ray differential equations.

datum surface, $x_3 = 0$, for the time-migrated data, we set $\gamma_1^0 = x_1^{M0}$, $\gamma_1^0 = x_2^{M0}$ as the horizontal coordinates of the starting point of the image ray. The given pair (x_1^{M0}, x_2^{M0}), also specifies the trace location in the time-migrated data set that corresponds to the image ray to be constructed. The initial traveltime of the image ray is $\gamma_3^0 = T^0 = 0$.

Since the initial slowness vector of an image ray, $\mathbf{p}^0$, is always perpendicular to the measurement surface, the two horizontal slowness vector components will both be zero, i.e., $p_1^0 = p_2^0 = 0$. The vertical slowness vector component is given by the inverse ray-domain velocity, $p_3^0 = 1/V_0$, at the trace location (x_1^{M0}, x_2^{M0}) and zero migration time, $t^{M0} = 2T^0 = 0$. Furthermore, one can show (Appendix E) that the factor F in equation 12 has the limit one when the migration time approaches zero; hence, equation 11 yields the initial ray-domain velocity as

$$V^0 = v_{dix}^M(\boldsymbol{\gamma}^0)\ . \tag{20}$$

Given the above specifications, the kinematic initial conditions for the image ray read

$$\mathbf{x}^0 = (x_1^{M0}, x_2^{M0}, 0)^T \quad \text{and} \quad \mathbf{p}^0 = (0, 0, \frac{1}{V^0})^T\ . \tag{21}$$

The initial unit vector ${\mathbf{e}_1}^0$ of the ray-centered coordinate system can be chosen quite freely within the horizontal plane. One option is to align it with the migration azimuth direction, in other words, to specify ${\mathbf{e}_1}^0 = (\cos\theta, \sin\theta, 0)^T$. The initial ray propagator matrix, $\mathbf{\Pi}^0$, is the 4×4 identity matrix given by equation 8.

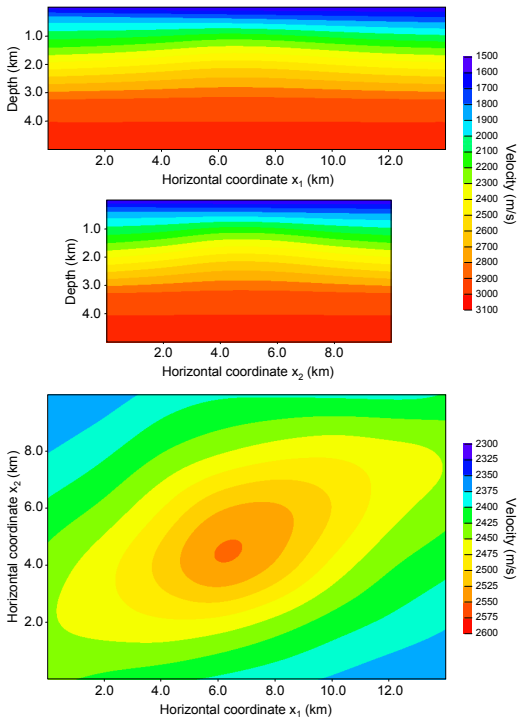

Figure 1: Left: Depth-domain velocity used for generating input data for the tests. Top: Section $x_2 = 5$ km. Middle: Section $x_1 = 7$ km. Bottom: Depth slice $x_3 = 2$ km

NUMERICAL EXAMPLES

In this section, we consider, as a first illustration of the method, examples based on a 3D model of the subsurface. Three cross-sections through the P-wave velocity field of this model are shown in Figure I. The velocity field contains mild lateral variations and is smooth throughout, i.e., it has no interfaces, discontinuities, or areas without data.

In order to obtain input data for the numerical tests, image rays were traced a one-way time $T = 2$ s downward from a planar measurement surface, located at depth $x_3 = 0$ km. Figure 2 (left) shows image rays projected into the three global Cartesian coordinate directions. One can observe deviations of rays from the vertical; still, the velocity variations responsible for these deviations do not introduce triplications and caustics in the image-ray field. To facilitate display and comparisons of velocities, positions, and their errors, we show, in the following, all results as functions of the coordinates of the time-migration domain. As an introduction to this type of display, consider Figure 2 (right), which shows the "true" depth-domain velocity posted along the generated image rays. By calculating the ray propagator matrix along the rays, we obtained, as a by-product, the matrix of second derivatives of the one-way diffraction time, which contains information about migration velocity for any azimuth, θ. Thereafter, we selected specifically the migration velocity field corresponding to the azimuth $\theta = 0$ degrees (Figure 3) (left) and converted it to a time-migration interval velocity field (Figure 3) (right), using Dix's method, see equation 2. The reason for calculating the input data in this way was to attain control of errors resulting from the image-ray transformation alone. We remark, in passing, that an equivalent approach to obtaining time-migration interval velocities is to use equation 38.

The experiments were conducted with two transformations relating the time and depth domains. One approach was established by neglecting all lateral variations of the time-migration interval velocity. Since this action results in vertical image rays, we refer to it as the *vertical-ray transformation*. The other approach is based on the methodology for the image-ray transformation presented in this paper, but with the underlying assumption that the derivatives of ray-centered coordinates along a ray, q_K, of higher order than one in the ray parameters, γ_I, can be neglected.

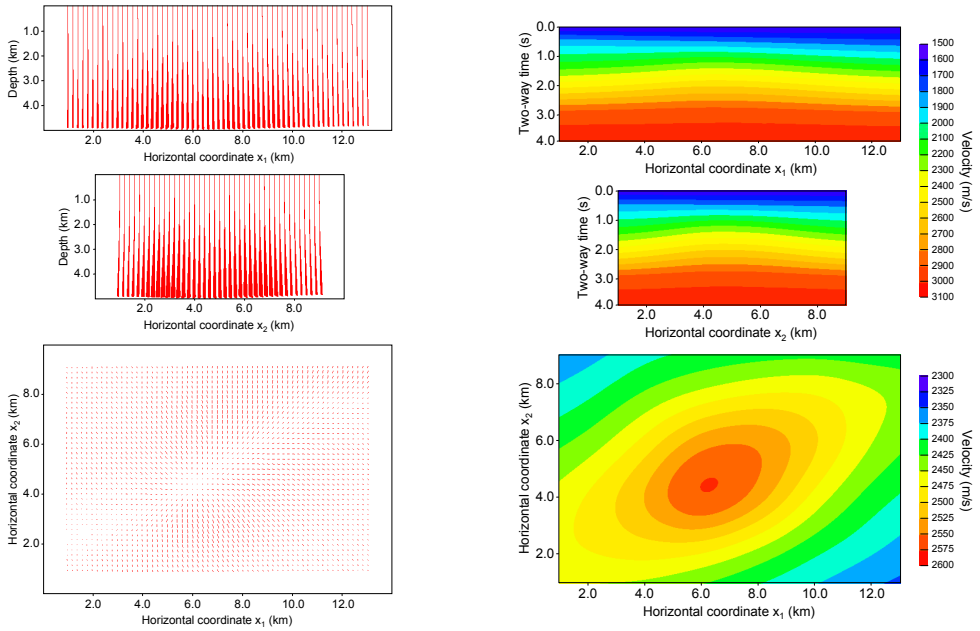

Figure 2: Left: Projections of image rays in (top) x_2 direction, (middle) x_1 direction, and (bottom) x_3 direction; Right: Depth-domain velocity as a function of time-domain coordinates. Top: Section $x_2 = 5$ km. Middle: Section $x_1 = 7$ km. Bottom: Time slice $T^M = 2$ s

Considering first the vertical-ray transformation, Figure 4 (left) shows errors in the estimation of the position (x_i) for a selected time slice, $T^M = 2$ s. The corresponding errors resulting from the image-ray transformation are shown in Figure 4 (right). The latter displays can be interpreted as estimated time-to-depth conversion errors for a virtual flat horizon in the time-migration domain. A possibility of direct comparison between the vertical-ray and image-ray transformations is provided in Figure 5 (left). It can be concluded that the errors arising from the applied image-ray transformation are smaller than those of the vertical-ray transformation, in particular what regards the error in lateral positioning. From Figure 5 (right) one can compare the accuracy of the depth-domain velocities obtained by the two approaches. Again, the image-ray transformation generally yields smaller errors. We remark, however, that this approach is quite sensitive to the smoothness of the first- and second-order derivatives of the time-migration interval velocity field.

CONCLUSIONS

Starting from a given three-dimensional time-migration velocity field, available for a single migration azimuth, we have presented an efficient scheme to trace image rays and simultaneously estimate the velocity along them. The obtained velocities can provide, after regularization, a depth-domain velocity field that can be useful for many seismic applications. These include, e.g., the use of the estimated velocity field as a macro-velocity model for depth migration or as an initial model for tomographic inversion. The proposed scheme also provides the basis for time-to-depth conversion without the need for a priori information of the depth-domain velocity model.

We have greatly benefited from recent investigations that establish the link between the time-migration interval velocity and the corresponding velocity along the image ray. The resulting algorithm for 3D image-ray tracing into depth uses a time-migration velocity field known in three different azimuths. In this paper, besides reviewing the literature, we have introduced an alternative algorithm, which requires the knowledge of the time-migration velocity field in a single azimuth only. As a consequence, we foresee that our approach will be easier to use in practice. The new algorithm has been applied and discussed on a 3D synthetic example. An overall impression from this first test is that the errors generated by the developed image-ray transformation are smaller than those of the classic vertical-ray transformation, in particular concerning lateral positioning.

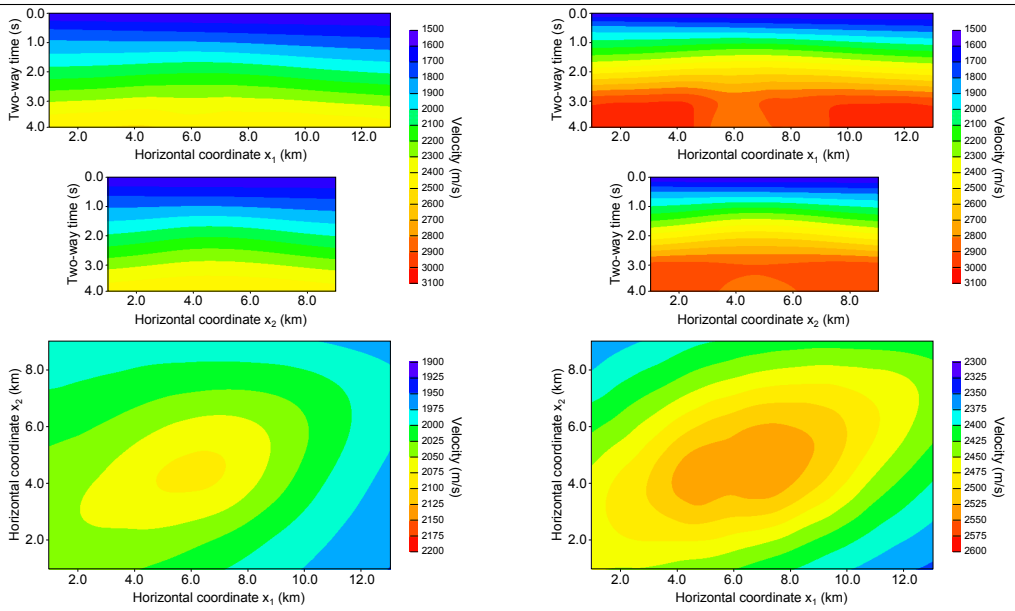

Figure 3: Left: Time-migration velocity as a function of time-domain coordinates. Top: Section $x_2^M = 5$ km. Middle: Section $x_1^M = 7$ km. Bottom: Time slice $T^M = 2s$; Right: Time-migration interval velocity as a function of time-domain coordinates. Top: Section $x_2^M = 5$ km. Middle: Section $x_1^M = 7$ km. Bottom: Time slice $T^M = 2$ s.

The present scheme is bound to yield best results whenever time migration provides sufficient focusing and also a reliable time-migration velocity field. As main advantage, it delivers a direct estimation of the depth-domain velocity, with a minimum of user interaction/intervention. The method is very efficient, as compared, for example, to full prestack depth migration and associated estimation of depth-domain velocity parameters. The constraints or limitations of the proposed procedure are the ones basically inherited by the use of time migration, the ray method, and Dix's type velocity inversions. For adequate ray-tracing implementation, the time-migration interval velocity function, as well as its first-and second-order derivatives, all need to be "sufficiently smooth". Moreover, the resolution in the velocity estimation is expected to be poor for deep and/or thin "layers". As an additional condition for effective implementation, care should be taken such that the image-ray field has no triplications and caustics.

ACKNOWLEDGMENTS

We thank F. Adler, I. Pšenčík, S. Fomel and J. A. Sethian for constructive criticism and helpful suggestions. E. Iversen acknowledges support from the *Research Council of Norway* (project 174549/S30), *StatoilHydro*, and *NORSAR*. In particular, he is grateful to his colleagues K. Åstebøl and H. Gjøystdal for a fruitful collaboration on the topic of time-to-depth conversion along image rays in the late 1980s. The work performed at that time was not published as a regular paper, but essential results were, however, presented to the EAEG meeting (Iversen et al., 1987) and in a NORSAR report (Iversen et al., 1988). M. Tygel acknowledges support from the *National Council of Scientific and Technological Development (CNPq)*, Brazil, the *Research Foundation of the State of São Paulo (FAPESP)*, Brazil. This work has also been supported by the sponsors of the *Wave Inversion Technology (WIT) Consortium*, Karlsruhe, Germany.

REFERENCES

Cameron, M. K., Fomel, S., and Sethian, J. A. (2006). Seismic velocity estimation and time to depth conversion of time-migrated images. In *76th Ann. Internat. Mtg., SEG, Abstracts*, pages 3066–3070.

Cameron, M. K., Fomel, S., and Sethian, J. A. (2007). Seismic velocity estimation from time migration. *Inverse Problems*, 23:1329–1369.

Iversen, E., Åstebøl, K., and Gjøystdal, H. (1987). Time-to-depth conversion of 3D seismic interpretation

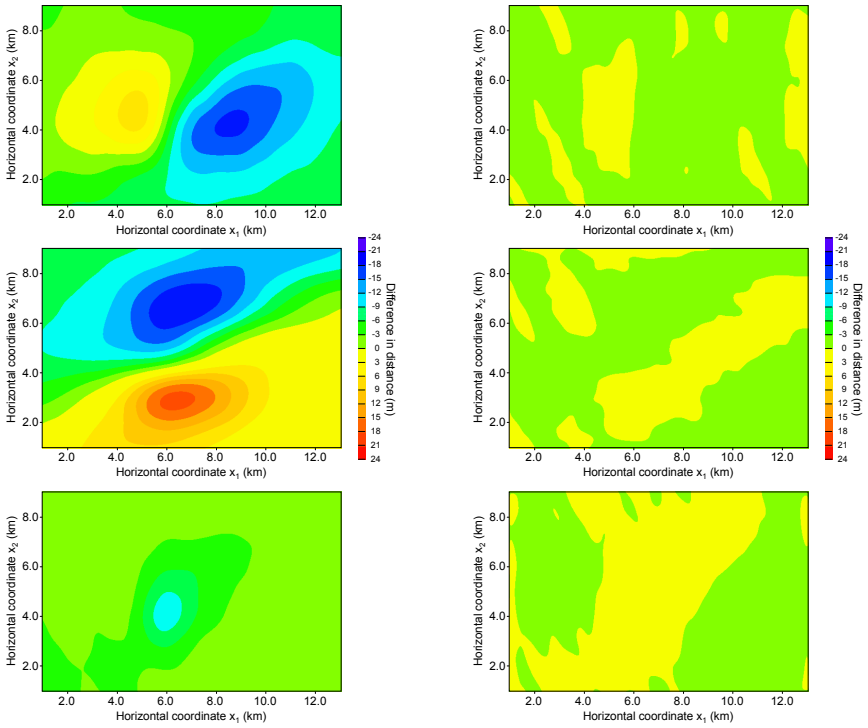

Figure 4: Left: Vertical-ray transformation: Depth-domain position errors for time slice $T^M = 2$ s. Coordinates (top) x_1, (middle) x_2, and (bottom) x_3; Right: Image-ray transformation approach: Depth-domain position errors for time slice $T^M = 2$ s. Coordinate errors (top) x_1, (middle) x_2, and (bottom) x_3.

data by use of 'dynamic image rays'. In *49th Ann. Internat. Mtg., Eur. Ass. of Expl. Geophys., Abstracts*, page 16.

Iversen, E., Åstebøl, K., and Gjøystdal, H. (1988). 3D time-to-depth conversion of interpreted time-migrated horizons by use of the paraxial image ray method. *Research report, NORSAR, Norway*.

Iversen, E. and Tygel, M. (2006). Time-to-depth mapping and imaging of time-migrated seismic data with inherent velocity estimation. *WIT Annual Report*, 10:92–106.

Popov, M. M. and Pšenčík, I. (1978). Computation of ray amplitudes in inhomogeneous media with curved interfaces. *Studia Geophysica et Geodaetica*, 22:248–258.

Červený, V. (2001). *Seismic Ray Theory*, page 768. Cambridge University Press.

APPENDIX A

COMPARISON WITH THE APPROACH OF CAMERON ET AL. (2007)

The time-to-depth conversion procedure presented in this paper is based on the knowledge of migration velocity, $V^M(\bar{\mathbf{x}}^M, T^M, \theta)$, corresponding to a single azimuth, θ. Cameron et al. (2007) presented a different time-to-depth conversion approach, relying on the complete information of the variation of migration velocity with azimuth. This information is contained in the matrix $\mathbf{M}^{(x)}(\bar{\mathbf{x}}^M, T^M)$. When matrix $\mathbf{M}^{(x)}$ is known for all relevant locations in the domain $(\bar{\mathbf{x}}^M, T^M)$, one can easily obtain the inverse matrix

$$\mathbf{N}^{(x)} = \mathbf{M}^{(x)^{-1}} , \tag{22}$$

as well as the derivatives

$$\mathbf{W} = \frac{d\mathbf{N}^{(x)}}{dT} = 2\frac{d\mathbf{N}^{(x)}}{dT^M} . \tag{23}$$

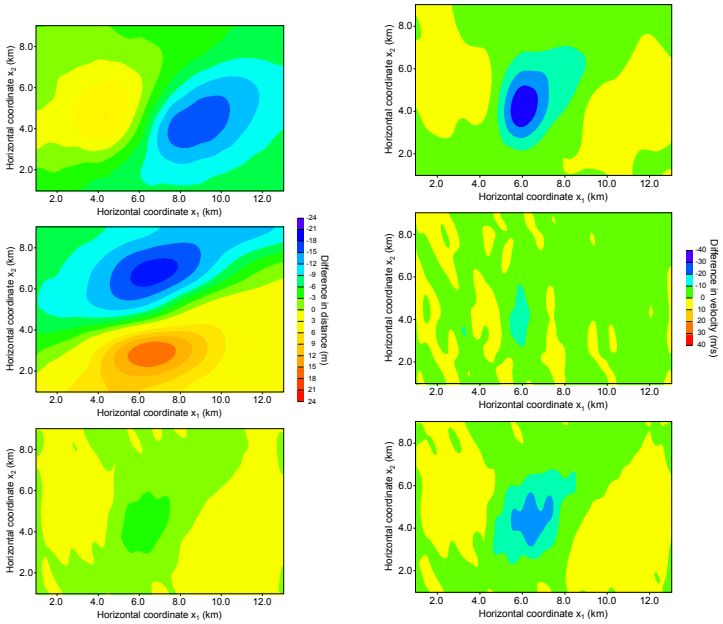

Figure 5: Left: Vertical-ray vs. image-ray transformation approaches: Depth-domain position differences for time slice $T^M = 2$ s. Differences in coordinates (top) x_1, (middle) x_2, and (bottom) x_3; Right: Comparisons of depth-domain velocities for time slice $T^M = 2$ s. Error using (top) vertical-ray and (middle) image-ray transformation. Bottom: Difference between the vertical-ray and image-ray transformations. The velocity differences in the top, middle, and bottom sub-figures correspond, respectively, to the position differences in Figures 7, 8, and 9.

Matrix $\mathbf{W}$, constituting the input data for the time-to-depth conversion in the approach of Cameron et al. (2007), is related to depth-domain velocity, V, and matrix $\mathbf{Q}_1^{\downarrow(x)}$ by (see their equation 27)

$$\mathbf{W} = V^2 \left(\mathbf{Q}_1^{\downarrow(x)^T} \mathbf{Q}_1^{\downarrow(x)} \right)^{-1} . \tag{24}$$

Introducing a unit azimuth direction vector, $\bar{\mathbf{u}}$, and using the above equation, one can write

$$V^2 = \bar{\mathbf{u}}^T \mathbf{W} \mathbf{E} \bar{\mathbf{u}} \, , \tag{25}$$

where matrix $\mathbf{E}$ is defined as

$$\mathbf{E} = \mathbf{Q}_1^{\downarrow(x)^T} \mathbf{Q}_1^{\downarrow(x)} . \tag{26}$$

Equation 25 can be compared to our result

$$V^2 = (v_{dix}^M)^2 F^2 . \tag{27}$$

Equations 25 and 27 represent two different bases for time-to-depth conversion and velocity estimation. The approach based on equation 25, described by Cameron et al. (2007), uses as input the matrix $\mathbf{W}$. The dynamic ray tracing required for calculation of matrix $\mathbf{E}$ involves calculation of matrices $\mathbf{Q}_1^{\downarrow}$ and $\mathbf{P}_1^{\downarrow}$, that means, calculation of the second set of paraxial matrices is not required. The approach described in this paper, which is based on equation 27, uses as input the time-migration interval velocity, v_{dix}^M, for a selected azimuth direction, $\bar{\mathbf{u}}$. The dynamic ray-tracing procedure needed for calculation of factor F, however, requires calculation of both sets of paraxial matrices, $(\mathbf{Q}_I, \mathbf{P}_I)$.

APPENDIX B

VELOCITY SPREADING FACTOR FOR THE IMAGE RAY

Derivations for velocity spreading along the image ray in the 2D and multi-azimuth 3D situations were given in Cameron et al. (2006, 2007). In this appendix, we derive equation 12 for the velocity spreading

factor, F, pertaining to the single-azimuth 3D case. Our starting point is the relationship between the (azimuth-dependent) migration velocity, $V^M(\bar{\mathbf{x}}^M, T^M, \theta)$, to the 2×2 matrix, $\mathbf{M}^{(x)}(\bar{\mathbf{x}}^M, T^M)$, of second derivatives of one-way, upward, traveltime. Introducing the one-way, downward, migrated time $T = T^M/2$, it is given by

$$T[V^M]^2 = \frac{1}{\bar{\mathbf{u}}^T \mathbf{M}^{(x)} \bar{\mathbf{u}}} \,, \tag{28}$$

where $\bar{\mathbf{u}}$ is the direction vector for the migration azimuth used to obtain the migration velocity, V^M. One can relate matrix $\mathbf{M}^{(x)}$ to the corresponding matrix $\mathbf{M}_2^{\uparrow}$ expressed in the ray-centered coordinates for the upward direction of the image ray, as follows,

$$\mathbf{M}^{(x)} = \mathbf{I}^* \mathbf{M}_2^{\uparrow} \mathbf{I}^* \,, \tag{29}$$

where

$$\mathbf{I}^* = \begin{pmatrix} -1 & 0 \\ 0 & 1 \end{pmatrix}. \tag{30}$$

Inserting $\mathbf{M}_2^{\uparrow} = \mathbf{P}_2^{\uparrow} {\mathbf{Q}_2^{\uparrow}}^{-1}$, and applying the relations for backward propagation of the ray propagator matrix in Iversen (2006), we obtain

$$\mathbf{M}^{(x)} = \mathbf{I}^* \left(\mathbf{I}^* {\mathbf{Q}_1^{\downarrow}}^T \mathbf{I}^* \right) \left(\mathbf{I}^* {\mathbf{Q}_2^{\downarrow}}^T \mathbf{I}^* \right)^{-1} \mathbf{I}^* = {\mathbf{Q}_1^{\downarrow}}^T {\mathbf{Q}_2^{\downarrow}}^{-T} = {\mathbf{Q}_2^{\downarrow}}^{-1} \mathbf{Q}_1^{\downarrow} \,. \tag{31}$$

The last operation is a consequence of the fact that matrix $\mathbf{M}^{(x)}$ is symmetric. Considering again equation 28, the migration velocity can therefore be calculated from the equation

$$T[V^M]^2 = \frac{1}{\bar{\mathbf{u}}^T {\mathbf{Q}_2^{\downarrow}}^{-1} \mathbf{Q}_1^{\downarrow} \bar{\mathbf{u}}} \,. \tag{32}$$

Substituting equation 32 into the Dix velocity equation 2, we obtain the important relation

$$(v_{dix}^M)^2 = \frac{d}{dT} \left[\frac{1}{\bar{\mathbf{u}}^T {\mathbf{Q}_2^{\downarrow}}^{-1} \mathbf{Q}_1^{\downarrow} \bar{\mathbf{u}}} \right] = - \frac{\bar{\mathbf{u}}^T \dfrac{d}{dt} [{\mathbf{Q}_2^{\downarrow}}^{-1} \mathbf{Q}_1^{\downarrow}] \bar{\mathbf{u}}}{\left[\bar{\mathbf{u}}^T {\mathbf{Q}_2^{\downarrow}}^{-1} \mathbf{Q}_1^{\downarrow} \bar{\mathbf{u}} \right]^2} \,. \tag{33}$$

To compute the derivative in the above equation, we observe that, for an isotropic medium, the differential equation for paraxial matrix $\mathbf{Q}_I^{\downarrow}$, for $I = 1, 2$, is

$$\frac{d\mathbf{Q}_I^{\downarrow}}{dT} = v^2 \mathbf{P}_I^{\downarrow} \quad \text{and also} \quad \frac{d{\mathbf{Q}_I^{\downarrow}}^{-1}}{dT} = - v^2 {\mathbf{Q}_I^{\downarrow}}^{-1} \mathbf{P}_I^{\downarrow} {\mathbf{Q}_I^{\downarrow}}^{-1} \,. \tag{34}$$

The rightmost equation was obtained under the application of the generic formula

$$\frac{d\mathbf{A}^{-1}}{dT} = - \mathbf{A}^{-1} \frac{d\mathbf{A}}{dT} \mathbf{A}^{-1} \,, \tag{35}$$

which results from differentiating both sides of the identity $\mathbf{A}^{-1}\mathbf{A} = \mathbf{I}$, followed by the application of the leftmost equation 34. Using the chain rule and also taking into account equations 34, we get

$$\begin{aligned} \frac{d}{dT} [{\mathbf{Q}_2^{\downarrow}}^{-1} \mathbf{Q}_1^{\downarrow}] &= V^2 \left[-{\mathbf{Q}_2^{\downarrow}}^{-1} \mathbf{P}_2^{\downarrow} {\mathbf{Q}_2^{\downarrow}}^{-1} \mathbf{Q}_1^{\downarrow} + {\mathbf{Q}_2^{\downarrow}}^{-1} \mathbf{P}_1^{\downarrow} \right] \\ &= - V^2 {\mathbf{Q}_2^{\downarrow}}^{-1} \left[\mathbf{P}_2^{\downarrow} {\mathbf{Q}_2^{\downarrow}}^{-1} - \mathbf{P}_1^{\downarrow} {\mathbf{Q}_1^{\downarrow}}^{-1} \right] \mathbf{Q}_1^{\downarrow} = - V^2 {\mathbf{Q}_2^{\downarrow}}^{-1} {\mathbf{Q}_2^{\downarrow}}^{-T} \,, \end{aligned} \tag{36}$$

where we have used the identity

$$\mathbf{P}_2^{\downarrow} {\mathbf{Q}_2^{\downarrow}}^{-1} - \mathbf{P}_1^{\downarrow} {\mathbf{Q}_1^{\downarrow}}^{-1} = {\mathbf{Q}_2^{\downarrow}}^{-T} {\mathbf{Q}_1^{\downarrow}}^{-1} \,, \tag{37}$$

which is a property of the ray propagator matrix (see, e.g., Červený, 2001, equations 4.3.16). Substitution into the Dix velocity formula 33 yields

$$(v_{dix}^M)^2 = V^2 \frac{\bar{\mathbf{u}}^T \mathbf{Q}_2^{\downarrow\,-1} \mathbf{Q}_2^{\downarrow\,-T} \bar{\mathbf{u}}}{\left[\bar{\mathbf{u}}^T \mathbf{Q}_2^{\downarrow\,-1} \mathbf{Q}_1^{\downarrow} \bar{\mathbf{u}}\right]^2} \,. \tag{38}$$

from which

$$F^2 = \frac{V^2}{(v_{dix}^M)^2} = \frac{[\bar{\mathbf{u}}^T \mathbf{Q}_2^{\downarrow\,-1} \mathbf{Q}_1^{\downarrow} \bar{\mathbf{u}}]^2}{\bar{\mathbf{u}}^T \mathbf{Q}_2^{\downarrow\,-1} \mathbf{Q}_2^{\downarrow\,-T} \bar{\mathbf{u}}} \,. \tag{39}$$

Extracting the square root from both sides yields equation 12 given in the main text.

APPENDIX C

RELATING THE DERIVATIVES OF VELOCITY IN RAY COORDINATES AND LOCAL CARTESIAN COORDINATES

As in the algorithm derived by Cameron et al. (2007), our scheme requires to connect the derivatives of velocity in ray and local Cartesian coordinates. More specifically, we need relations between the derivatives of the velocity functions $V(\gamma_1, \gamma_2, \gamma_3)$ and $V(q_1, q_2, q_3)$. First-order derivatives in the two coordinate systems are connected by

$$\frac{\partial V}{\partial \gamma_i} = \frac{\partial q_k}{\partial \gamma_i} \frac{\partial V}{\partial q_k} \,. \tag{40}$$

Further differentiation yields

$$\frac{\partial^2 V}{\partial \gamma_i \partial \gamma_j} = \frac{\partial q_k}{\partial \gamma_i} \frac{\partial q_l}{\partial \gamma_j} \frac{\partial^2 V}{\partial q_k \partial q_l} + \frac{\partial^2 q_k}{\partial \gamma_i \partial \gamma_j} \frac{\partial V}{\partial q_k} \,. \tag{41}$$

We multiply both sides of equation 41 by the derivatives $(\partial \gamma_i / \partial q_n)$ and $(\partial \gamma_j / \partial q_m)$. The result is

$$\frac{\partial^2 V}{\partial q_n \partial q_m} = \frac{\partial \gamma_i}{\partial q_n} \frac{\partial \gamma_j}{\partial q_m} \left(\frac{\partial^2 V}{\partial \gamma_i \partial \gamma_j} - \frac{\partial^2 q_k}{\partial \gamma_i \partial \gamma_j} \frac{\partial V}{\partial q_k} \right) \,. \tag{42}$$

The derivatives needed specifically for dynamic ray tracing are $\partial^2 V / \partial q_N \partial q_M$. Utilizing that $\partial \gamma_3 / \partial q_N = 0$ and that $\partial V / \partial q_3 = V^{-1} \partial V / \partial T$, we obtain

$$\frac{\partial^2 V}{\partial q_N \partial q_M} = \frac{\partial \gamma_I}{\partial q_N} \frac{\partial \gamma_J}{\partial q_M} \left(\frac{\partial^2 V}{\partial \gamma_I \partial \gamma_J} - \frac{\partial^2 q_K}{\partial \gamma_I \partial \gamma_J} \frac{\partial V}{\partial q_K} \right) - V^{-1} \frac{\partial \gamma_I}{\partial q_N} \frac{\partial \gamma_J}{\partial q_M} \frac{\partial^2 q_3}{\partial \gamma_I \partial \gamma_J} \frac{\partial V}{\partial T} \,. \tag{43}$$

In a similar way as for velocity, V, one can relate derivatives of traveltime, T, in ray coordinates and local Cartesian coordinates, as follows,

$$\frac{\partial T}{\partial \gamma_i} = \frac{\partial q_k}{\partial \gamma_i} \frac{\partial T}{\partial q_k} \,, \tag{44}$$

$$\frac{\partial^2 T}{\partial \gamma_i \partial \gamma_j} = \frac{\partial q_k}{\partial \gamma_i} \frac{\partial q_l}{\partial \gamma_j} \frac{\partial^2 T}{\partial q_k \partial q_l} + \frac{\partial^2 q_k}{\partial \gamma_i \partial \gamma_j} \frac{\partial T}{\partial q_k} \,. \tag{45}$$

In the following, we consider only the ray coordinates γ_I. Moreover, we utilize that traveltime T is constant along a wavefront, which means that $\partial T / \partial q_K = 0$ and $\partial^2 T / \partial \gamma_I \partial \gamma_J = 0$. Consequently, equation 45 can be restated as

$$0 = \frac{\partial q_K}{\partial \gamma_I} \frac{\partial q_L}{\partial \gamma_J} \frac{\partial^2 T}{\partial q_K \partial q_L} + \frac{\partial^2 q_3}{\partial \gamma_I \partial \gamma_J} \frac{\partial T}{\partial q_3} \,. \tag{46}$$

Applying the definition $M_{KL} = \partial^2 T / \partial q_K \partial q_L$, and inserting $\partial T / \partial q_3 = V^{-1}$, we obtain,

$$\frac{\partial^2 q_3}{\partial \gamma_I \partial \gamma_J} = -V \frac{\partial q_K}{\partial \gamma_I} \frac{\partial q_L}{\partial \gamma_J} M_{KL} \,. \tag{47}$$

The last result is substituted into equation 43, which yields

$$\frac{\partial^2 V}{\partial q_N \partial q_M} = \frac{\partial \gamma_I}{\partial q_N}\frac{\partial \gamma_J}{\partial q_M}\left(\frac{\partial^2 V}{\partial \gamma_I \partial \gamma_J} - \frac{\partial^2 q_K}{\partial \gamma_I \partial \gamma_J}\frac{\partial V}{\partial q_K}\right) + M_{NM}\frac{\partial V}{\partial T}\ . \tag{48}$$

Therefore, for a situation where the effect of the derivatives $\partial^2 q_K/\partial\gamma_I\partial\gamma_J$ is negligible, we can use, in matrix form, the approximation

$$\frac{\partial^2 V}{\partial \bar{\mathbf{q}}^2} = \mathbf{Q}_1^{-T}\frac{\partial^2 V}{\partial \bar{\boldsymbol{\gamma}}^2}\mathbf{Q}_1^{-1} + \mathbf{M}_1\frac{\partial V}{\partial T}\ , \tag{49}$$

where $\mathbf{M}_1 = \mathbf{P}_1\mathbf{Q}_1^{-1}$.

APPENDIX D

COMPUTATION OF VELOCITY DERIVATIVES ALONG THE IMAGE RAY

In this appendix, we describe an approach for computation of the first and second derivatives, $\partial V/\partial\boldsymbol{\gamma}$ and $\partial^2 V/\partial\boldsymbol{\gamma}^2$ at each ray coordinate vector, $\boldsymbol{\gamma}$, that are required for our image-ray tracing scheme. Twice differentiation of equation 11 yields

$$\frac{\partial V}{\partial \gamma_i} = \frac{\partial v_{dix}^M}{\partial \gamma_i}\ F + v_{dix}^M\frac{\partial F}{\partial \gamma_i} \tag{50}$$

and

$$\frac{\partial^2 V}{\partial \gamma_i \partial \gamma_j} = \frac{\partial^2 v_{dix}^M}{\partial \gamma_i \partial \gamma_j}\ F + \left[\frac{\partial v_{dix}^M}{\partial \gamma_i}\ \frac{\partial F}{\partial \gamma_j} + \frac{\partial v_{dix}^M}{\partial \gamma_j}\ \frac{\partial F}{\partial \gamma_i}\right] + v_{dix}^M\ \frac{\partial^2 F}{\partial \gamma_i \partial \gamma_j}\ . \tag{51}$$

Since v_{dix}^M and its derivatives are known, our problem reduces to finding the derivatives of the velocity-spreading factor F, given by equation 12. The factor F depends on the matrices $\mathbf{Q}_1$ and $\mathbf{Q}_2$ of the dynamic ray-tracing system. In view of the discussion related to equation 18, it is clear that for a time-to-depth-conversion procedure based on tracing single image rays, one has to make the approximation that the derivatives of factor F with respect to γ_I, along a given ray, are neglected. As a consequence, only the derivatives in equations 50-51 of F with respect to T survive.

One can show, finally, that our integration procedure does not rely on the second derivatives $\partial^2 V/\partial T^2$, which means that calculation of the second derivative $\partial^2 F/\partial T^2$ is not required. Equations 50-51 can therefore be restated as

$$\frac{\partial V}{\partial \gamma_I} = \frac{\partial v_{dix}^M}{\partial \gamma_I}\ F\ , \quad \frac{\partial V}{\partial T} = \frac{\partial v_{dix}^M}{\partial T}\ F + v_{dix}^M\frac{\partial F}{\partial T} \quad \text{and} \quad \frac{\partial^2 V}{\partial \gamma_I \partial \gamma_J} = \frac{\partial^2 v_{dix}^M}{\partial \gamma_I \partial \gamma_J}\ F\ . \tag{52}$$

Given the above approximations, we are reduced, thus, to the calculation of $\partial F/\partial T$. For that matter, it is convenient to introduce the quantities

$$A = \bar{\mathbf{u}}^T\mathbf{Q}_2^{-1}\mathbf{Q}_1\bar{\mathbf{u}} \quad \text{and} \quad B = \bar{\mathbf{u}}^T\mathbf{Q}_2^{-1}\mathbf{Q}_2^{-T}\bar{\mathbf{u}}\ , \tag{53}$$

from which we can write F and $\partial F/\partial T$ as (see equation 12)

$$F = \frac{A}{B^{1/2}} \quad \text{and} \quad \frac{\partial F}{\partial T} = \frac{\partial A}{\partial T}\ B^{1/2} - \frac{A}{2B^{3/2}}\ \frac{\partial B}{\partial T}\ . \tag{54}$$

It remains to obtain $\partial A/\partial T$ and $\partial B/\partial T$. Working similarly to the derivation of equation 36, we readily find

$$\frac{\partial A}{\partial T} = -\,V^2\bar{\mathbf{u}}^T\mathbf{Q}_2{}^{-1}\mathbf{Q}_2{}^{-T}\bar{\mathbf{u}} = -\,V^2\,B \quad \text{and} \quad \frac{\partial B}{\partial T} = -\,2V^2\bar{\mathbf{u}}^T\mathbf{Q}_2{}^{-1}\mathbf{P}_2\mathbf{Q}_2{}^{-1}\mathbf{Q}_2{}^{-T}\bar{\mathbf{u}}\ . \tag{55}$$

It must be noted that the above formulas for factor F and its derivative $\partial F/\partial T$ cannot be used for zero migration time, for which $B = 0$. We find, however, that a second-order approximation for the factor F in the vicinity of $T = 0$ is given by

$$F = 1 - \frac{1}{2}VT^2\bar{\mathbf{u}}^T\frac{\partial^2 V}{\partial \bar{\boldsymbol{\gamma}}^2}\bar{\mathbf{u}}\ , \tag{56}$$

which yields, at $T = 0$,

$$F = 1 \ , \qquad \frac{\partial F}{\partial T} = 0 \ . \tag{57}$$

In the 2D situation, we have

$$F = Q_1 \ , \qquad \frac{\partial F}{\partial T} = \frac{dQ_1}{dT} = V^2 P_1 \ , \tag{58}$$

which is reduced to equation 57 in the limit of zero time, since at that time $Q_1 = 1$ and $P_1 = 0$.